

# EFFECT OF HIGH ENERGY ELECTRON BEAM IRRADIATION ON THE OPTICAL PROPERTIES OF NANOCRYSTALLINE TiO<sub>2</sub>

K. P. Priyanka<sup>1</sup>, Sunny Joseph<sup>1</sup>, AnuTresa Sunny<sup>2</sup>, Thomas Varghese<sup>1\*</sup>

<sup>1</sup>Nanoscience Research Centre (NSRC), Dept. of Physics, Nirmala College,  
Muvattupuzha - 686 661, Kerala, India

<sup>2</sup>School of Chemical Sciences, Mahatma Gandhi University,  
Kottayam - 686 560, Kerala, India

\*nanoncm@gmail.com

The effect of high energy electron beam irradiation on the optical properties of TiO<sub>2</sub> nanoparticles was studied in order to improve the optical absorption performance and photo-activity. Electron beam irradiation may have resulted in size reduction, which in turn caused an increase of the optical band gap and photoluminescence intensity. Irradiation at a suitable dose rate was found to enhance the optical absorption performance and photo-activity of the tested TiO<sub>2</sub> nanoparticles.

**Keywords:** TiO<sub>2</sub>, electron beam irradiation, optical properties, photoluminescence.

## 1. Introduction

Nanocrystalline TiO<sub>2</sub> is a well-known semiconductor with photocatalytic activities, having great potential as photoelectric converters with applications in solar cells, environmental purification and for the generation of hydrogen gas. TiO<sub>2</sub> exists in three polymorphic phases: rutile (tetragonal, density = 4.25 g/cm<sup>3</sup>), anatase (tetragonal, 3.894 g/cm<sup>3</sup>) and brookite (orthorhombic, 4.12 g/cm<sup>3</sup>). The low-density solid phases are less stable and undergo transition to rutile in the solid state. The transformation is accelerated by thermal treatment and occurs at temperatures between 450–1200 °C. This transformation is dependent on several parameters, such as initial particle size, initial phase, dopant concentration, reaction atmosphere and annealing temperature [1–5].

The absorption spectrum of a semiconductor defines its possible uses. The useful semiconductors for photocatalysis have a band gap comparable to the energy of the photons of visible light, having a value of  $E_g < 3.0$  eV.  $E_g$  value ranges from 2.86 to 3.34 eV have been reported in the literature for the anatase phase. Thus, TiO<sub>2</sub> would prove to be the most efficient if it would exhibit the unique ability to absorb visible light significantly. Unfortunately, however, TiO<sub>2</sub> is a poor visible light absorber, requiring a large band gap energy (3.2 eV) for the excitation of electrons from the filled valence band to the vacant conduction band. In order to enhance the photo-response and the photo-activity of TiO<sub>2</sub>, a variety of approaches have been employed: e.g. (i) doping with transition metals or nonmetals into TiO<sub>2</sub>, (ii) reducing TiO<sub>2</sub> using hydrogen plasma, (iii) adsorbing metal complexes or organic dyes onto the surfaces of TiO<sub>2</sub> [6–9] and (iv) high energy electron beam irradiation of TiO<sub>2</sub> nanoparticles [10].

The sol-gel method [11] is one of the most suitable routes to synthesize various metal oxides due to low cost, ease of fabrication and low reaction temperatures. This method is widely used to fabricate TiO<sub>2</sub> for films, particles or monoliths. The optimum fabrication conditions are provided for the narrow size distribution of the nanocrystalline TiO<sub>2</sub>. In this work, the sol-gel synthesis route has been employed for the preparation of TiO<sub>2</sub> nanoparticles.

The prepared TiO<sub>2</sub> nanoparticles were characterized by x-ray diffraction (XRD), transmission electron microscopy (TEM), UV-Visible and photoluminescence (PL) spectroscopy. In addition, the optical properties of the synthesized nanocrystalline TiO<sub>2</sub> samples and the electron beam irradiated samples were evaluated in context of the band gap.

## 2. Materials and Methods

Titanium (IV)-n-butoxide (Ti(OBu)<sub>4</sub>) (98%, Alfa Aesar), isopropyl alcohol (99%, Fisher Scientific) and HNO<sub>3</sub> (Merck) were used without further purification for the synthesis of nanocrystalline TiO<sub>2</sub>. Distilled water was used in all synthesis procedures.

The scheme for preparing the nanocrystalline TiO<sub>2</sub> used in this work has been presented schematically as shown in fig. 1. The precursor solution was a mixture of 5 ml titanium (IV)-n-butoxide (Ti(OBu)<sub>4</sub>) and 10 ml isopropyl alcohol. This solution was then added dropwise to a pH 2 solution of HNO<sub>3</sub>. The hydrolysis was performed at room temperature while stirring for 3 hours. After complete consumption of Ti(OBu)<sub>4</sub>, the solution was refluxed at 70 °C for 20 hours and a sol was formed. Finally, the formed sol was dried at 60 °C for 36 hours to obtain TiO<sub>2</sub> powders. The obtained powder samples were calcined for 3 hours in a furnace at 300–800 °C in an aerobic atmosphere.

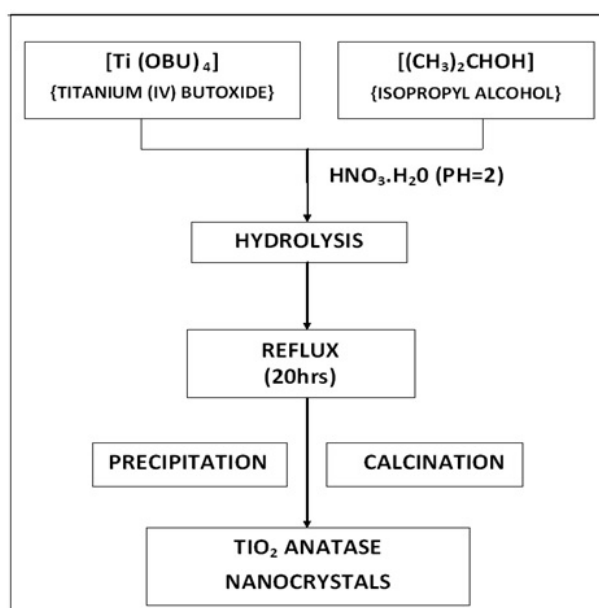


FIG. 1. The scheme of preparation of nanotitania by sol-gel method

The 800 °C calcined TiO<sub>2</sub> nanoparticles were irradiated with an 8 MeV electron beam obtained from a variable energy Microtron, (Department of Physics, Mangalore University, Mangalagangothri, Karnataka State). The rutile samples of TiO<sub>2</sub> nanoparticles were irradiated at a dose rate of 0.5, 1.5, 2.5 and 3.5 kGy, and characterized by UV-Visible absorption spectroscopy and PL spectroscopy. It is of interest to note that the samples with 2.5 and 3.5 kGy dose rates had significant modifications on both their UV and PL spectra.

The structural characteristics of the synthesized titania nanoparticles were also studied by X-ray powder diffraction using a Bruker D8 Advance X-ray diffractometer ( $\lambda = 1.5406 \text{ \AA}$ ) with Cu-K $\alpha$  radiation in  $2\theta$  range from 20 ° to 70 °. From the X-ray diffraction analysis all the peaks of pure TiO<sub>2</sub>, were well matched with the X-ray pattern of JCPDS Card No. 21-1272. These analyses were performed to determine both the crystal phase and the average crystallite size.

The latter value was estimated from the Debye–Scherrer equation [11]. The Debye–Scherrer equation is given by

$$t = 0.9\lambda/\beta \cos \theta, \quad (1)$$

where  $\lambda$  is the X-ray wavelength,  $\beta$  is the full width at half maximum (FWHM) of the peak and  $\theta$  is the Bragg's angle.

Transmission electron microscopy is a unique tool to get a direct image of the nanoparticles, revealing the distribution in the nanocrystal and on its surface. High magnification imaging with lattice contrast allows the determination of individual crystal morphology. For TEM studies, the TiO<sub>2</sub> powder was dispersed in ethanol using an ultrasonic bath. A drop of the suspension was placed on a copper grid coated with carbon film. After drying, the copper grid containing the nanoparticles was placed on a holder for the imaging process. TEM photographs of the prepared nanocrystalline rutile TiO<sub>2</sub> powder samples were taken using a Tecnai 30 G2 S-twin (model), FEI make 300 KV High Resolution Transmission Electron Microscope (HRTEM). The TEM images in fig. 2 provide good reviews of the sample surface.

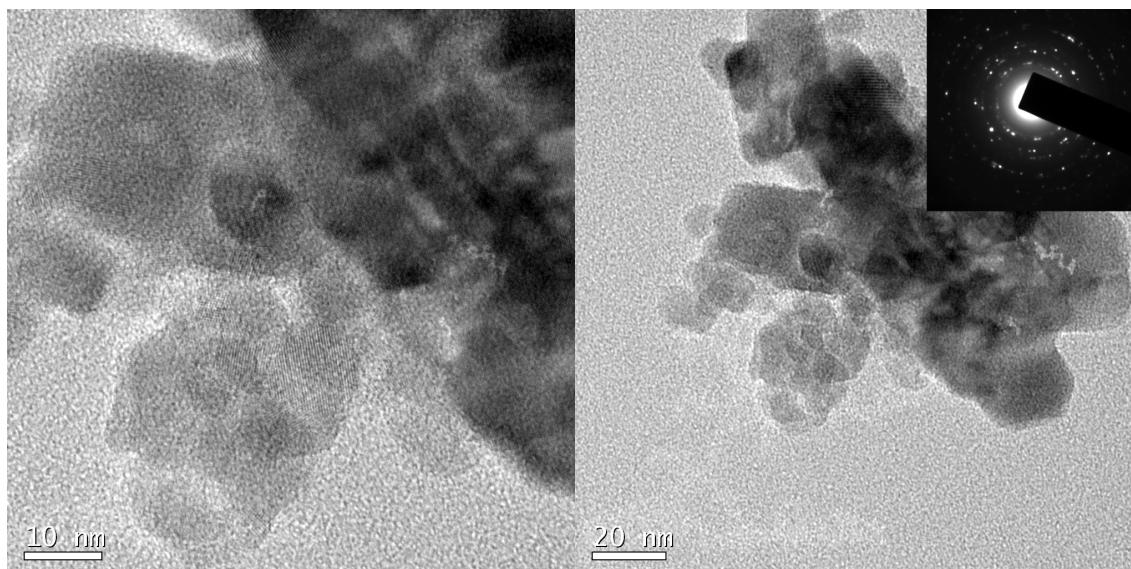


FIG. 2. TEM images of TiO<sub>2</sub> nanoparticles calcined at 800 °C

The absorption spectra of the pure and irradiated samples were recorded with a Shimadzu UV-Visible Spectrophotometer-UV 2600 model with ISR attachment. For measurement, the nanoparticles were pressed into a thick pellet, and placed at the entrance port of the integrating sphere using a sample holder. Calibration of the absorbance scale was done using standard reference materials. The wavelengths tested ranged from 200–800 nm.

Photoluminescence spectroscopy is an effective way to investigate the electronic structure and optical characteristics of semiconductor nanomaterials. This analytical technique reveals information such as surface defects and oxygen vacancies as well as the separation and recombination of photo-induced charge carriers [12]. Photoluminescence spectra were measured at room temperature by a Fluoromax-3 spectrophotometer. The effect of electron beam irradiation on PL spectra was investigated. The photo activity of electron beam irradiated TiO<sub>2</sub> samples can be evaluated by the measurement of PL spectra, since stronger PL intensities were associated with higher photo activities.

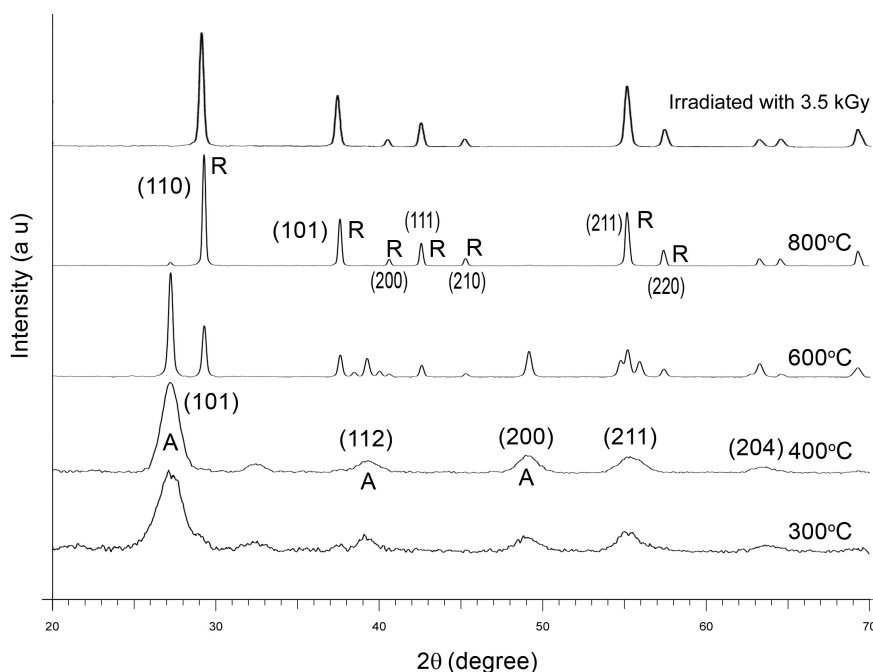


FIG. 3. The XRD spectra of TiO<sub>2</sub> nanoparticles calcined at different temperatures (A – Anatase; R – Rutile)

### 3. Results and Discussion

Figure 3 shows the X-ray diffraction patterns of uncalcined and calcined TiO<sub>2</sub> samples (A – anatase, R – rutile). The XRD pattern of the sample calcined at 300 °C revealed the presence of the anatase phase. Above 400 °C rutile peaks started to appear and a mixture of both the anatase and rutile phases of TiO<sub>2</sub> existed up to 800 °C. When the calcination temperature was 600 °C, sharp peaks associated with the rutile phase were observed. This suggests that there was a phase transition from anatase to rutile at temperatures lower than 600 °C. The residual anatase phase still exists in the samples up to 800 °C. At 800 °C, the transition to the rutile phase is almost complete. Fig. 3 shows that the diffraction peaks become intense and their FWHM gradually decreases with increasing calcination temperatures, verifying the increase in both the particle size and pertinent phase. The crystallite size obtained using equation (1) was 6 nm in the case of anatase TiO<sub>2</sub> calcined at 400 °C and 33 nm in the case of rutile TiO<sub>2</sub> calcined at 800 °C.

TEM was used to further examine the particle size, crystallinity and morphology of titania samples. TEM bright field images of TiO<sub>2</sub> nanoparticles in rutile (calcined at 800 °C) phase are shown in fig. 2. The TEM image revealed that particles were spherical or near-spherical in shape. Selected area electron diffraction (SAED) is shown in the inset of fig. 2, which clearly indicates that the TiO<sub>2</sub> nanoparticles were highly crystalline in nature. As can be seen from the TEM image, the average particle size is about 30 nm, which is in agreement with the crystallite size obtained from XRD data.

Figure 4 shows the UV-Visible absorbance spectra of pure and irradiated samples of rutile TiO<sub>2</sub> nanoparticles. S1 is pure sample, S2 and S3 are irradiated rutile samples at a dose rate of 2.5 kGy and 3.5 kGy respectively. The figure shows that the absorbance spectrum of rutile TiO<sub>2</sub> is shifted to the blue region, attributed to the quantum size effect [9]. Similar observations were reported for anatase TiO<sub>2</sub> samples [10]. The band gap values obtained for rutile samples

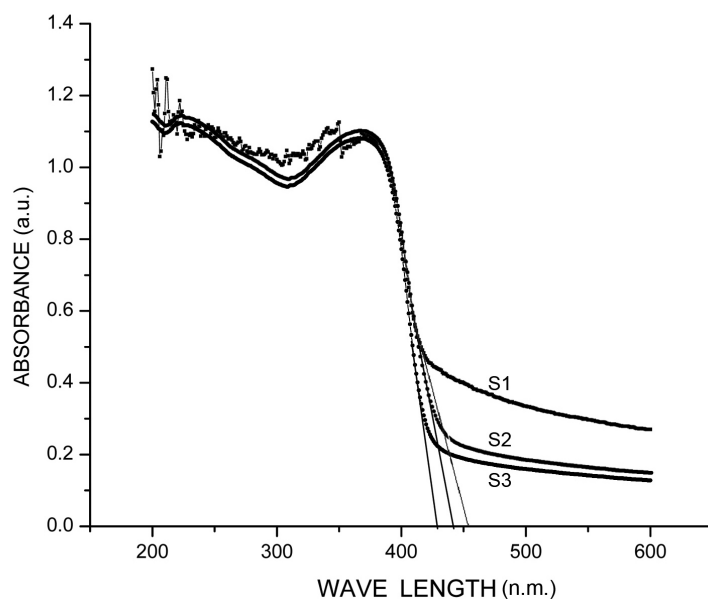


FIG. 4. UV-Vis absorption spectra of rutile  $\text{TiO}_2$  samples

were 2.81 eV (S1), 2.85 eV (S2) and 2.88 eV (S3) respectively. This increase in the band gap might occur due to size reduction of the nanoparticles resulting from electron beam irradiation. An additional advantage of size reduction is that the large surface area to volume ratio makes possible timely utilization of photogenerated carriers in interfacial processes [10]. Moreover, beam irradiation appeared to improve the optical absorption performance of  $\text{TiO}_2$  nanoparticles. In addition, both non- and irradiated  $\text{TiO}_2$  nanoparticles were useful for photocatalytic activities because their band gap energy values were comparable to the energy of visible or UV light photons. As a result, these materials may be well-suited for the fabrication of efficient solar cells.

Figure 5 shows the room temperature photoluminescence emission spectra of pure and irradiated samples of rutile  $\text{TiO}_2$  nanoparticles. S1 is pure rutile  $\text{TiO}_2$ , S2 and S3 are irradiated rutile samples with dose rates of 2.5 kGy and 3.5 kGy respectively. The rutile  $\text{TiO}_2$  nanoparticles exhibited a strong and wide PL signal at 400–500 nm with the excited wavelength of 300 nm as shown in fig. 5. The figure shows two obvious PL peaks at about 420 and 485 nm respectively. The former peak will be mainly resulting from band edge free excitons and the latter a result of binding excitons [13]. Both pure and irradiated  $\text{TiO}_2$  nanoparticles could exhibit obvious PL signal with similar curve shapes. However, there was a small blue shift in the case of irradiated samples because the electron beam irradiation might result in a slight reduction in particle size. The decrease in particle size had an obvious effect, increasing the surface energy, which can be attributed to the quantum confinement [14, 15]. As a result, a slight blue shift ( $\approx 0.0139$  eV) in the emission peak was observed. The PL spectra of irradiated samples were shown to have much larger intensities relative to non-irradiated samples. Sample S3, which was irradiated at 3.5 kGy, showed a large intensity PL spectrum. However, Jun and co-workers reported that the PL intensity decreased with beam irradiation [16]. The increase in PL intensity for an irradiated sample is attributed to the recombination of self-trapped excitons, which is a combined effect of defect centers generated by oxygen vacancies, small particle size, growth of the brookite phase and increased absorption over the UV and visible range [17]. The increase in PL intensity is an

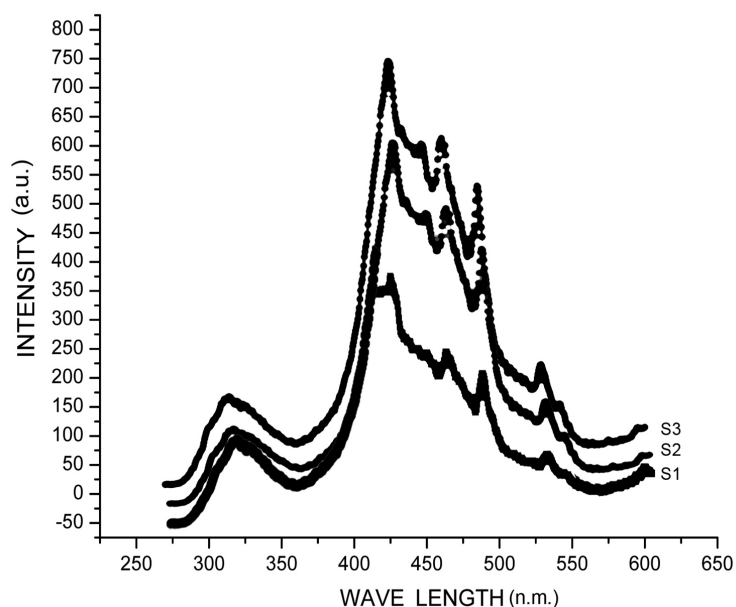


FIG. 5. Room temperature PL spectra of rutile TiO<sub>2</sub> samples

indication of higher photocatalytic activity. Moreover, the beam irradiation with suitable dose rate can help to enhance the photo-activity of TiO<sub>2</sub> nanoparticles. Similar observations have been reported for anatase TiO<sub>2</sub> nanoparticles [10].

#### 4. Conclusion

TiO<sub>2</sub> nanoparticles were synthesized by the sol-gel method and then irradiated with high energy electron beams. The optical properties of the pure and the beam-irradiated samples of rutile TiO<sub>2</sub> were investigated in context of the band gap. The absorption spectra of the irradiated samples were shifted to the blue region, which was attributed to the quantum size effect. The band gap obtained for the irradiated rutile TiO<sub>2</sub> samples were larger as compared to their pure samples. This increase of band gap might occur due to size reduction of the nanoparticles caused by the beam irradiation. The PL intensity of the irradiated samples was more, which was thought to arise from defects and particle size variation. Furthermore, the data obtained here would seem to show that the high energy electron beam irradiation at a suitable dose rate helps to enhance the optical response and photo-activity of TiO<sub>2</sub> nanoparticles.

#### Acknowledgments

The authors acknowledge their thanks to Nirmala College, Muvattupuzha and Microtron Centre, Mangalore University, Mangalore, Karnataka State for providing the opportunity to undertake this study. The financial support of this work by the KSCSTE, Thiruvananthapuram is gratefully acknowledged.

#### References

- [1] W. Li, S.I. Shah, et al. Metalorganic chemical vapor deposition and characterization of TiO<sub>2</sub> nanoparticles. *Mater. Sci. Eng. B*, **96**, P. 247 (2002).
- [2] E. Traversa. Design of ceramic materials for chemical sensors with novel properties. *J. Am. Ceram. Soc.*, **78** (1995).

- [3] H. Zhang, J.F. Banfield. Thermodynamic analysis of phase stability of nanocrystalline titania. *J. Mater. Chem.*, **8**, P. 2073–2076 (1998).
- [4] H.Z. Zhang, J.F. Banfield. Understanding Polymorphic Phase Transformation Behavior during Growth of Nanocrystalline Aggregates: Insights from TiO<sub>2</sub>. *J. Phys. Chem. B*, **104**, P. 3481 (2000).
- [5] A. Tsevis, N. Spanos, et al. Preparation and characterization of anatase powders. *J. Chem. Soc. Faraday Trans.*, **94**, P. 295–300 (1998).
- [6] S. Sahni, B. Reddy, B. Murty. Influence parameters on the synthesis of nano-titania by sol-gel route. *Mater. Sci. Eng. A*, **452–453**, P. 758–62 (2007).
- [7] F. Hossain, L. Sheppard, J. Nowotny, G. Murch. Optical properties of anatase and rutile titanium dioxide: Ab initio calculations for pure and anion-doped material. *J Phys. Chem. Solids*, **69**, P. 1820–8 (2008).
- [8] L. Palmisano, V. Augugliaro, A. Sclafani, M. Schiavello. Activity of chromium-ion-doped titania for the dinitrogen photoreduction to ammonia and for the phenol photodegradation. *J. Phys. Chem.*, **92**, P. 6710 (1998).
- [9] L.Q. Jing, Z.L. Xu, et al. The surface properties and photocatalytic activities of ZnO ultrafine particles. *Appl. Surf. Sci.*, **180**, P. 308–314 (2001).
- [10] K.P. Priyanka, Sunny Joseph, et al. Surface Modification of Nanotitania Using High Energy Electron Beam Irradiation. *Int. J. Emerg. Tech. Appl. Engg.*, **2** (11), P. 130–134 (2012).
- [11] T. Varghese, K.M. Balakrishna. *Nanotechnology: An introduction to synthesis, properties and applications*. Atlantic Publishers, New Delhi, P. 93–96 (2011).
- [12] W.F. Zhang, M.S. Zhang, Z.Yin, Q. Chen. Photoluminescence in anatase titanium dioxide nanocrystals. *Appl. Phys. B*, **70**, P. 261–265 (2000).
- [13] W.Li, C.Ni, et al. Size dependence of thermal stability of TiO<sub>2</sub> nanoparticles. *J. Appl. Phys.*, **96** (11), P. 6663 (2004).
- [14] J. Liqiang, S. Xiaojun, et al. The preparation and characterization of La doped TiO<sub>2</sub> nanoparticles and their photocatalytic activity. *J. Solid State Chem.*, **177**, P. 3375–3382 (2004).
- [15] H.K. Bo, H.K. Chang, et al. Electron beam irradiation effect on the photocatalytic activity of TiO<sub>2</sub> on carbon nanofibers. *J. Nanosci. Nanotech.*, **11**, P. 1438–1442 (2011).
- [16] J. Jun, J.H. Shin, J.S. Choi, M. Dhayal. Surface Modification of TiO<sub>2</sub> nanoparticles using electron beam radiation. *J. Biom. Nano*, **2** (2), P. 152–156 (2006).
- [17] S. K. Gupta, Rucha Desai, et al. Titanium dioxide synthesized using titanium chloride: size effect study using Raman spectroscopy and photoluminescence. *Journal of Raman Spectroscopy*, **41** (3), P. 350–355 (2010).